



Novel Technique for Visualizing Primordial Germ Cells in Sturgeons (*Acipenser ruthenus*, *A. gueldenstaedtii*, *A. baerii*, and *Huso huso*) 1

Authors: Saito, Taiju, and Psenicka, Martin

Source: Biology of Reproduction, 93(4)

Published By: Society for the Study of Reproduction

URL: <https://doi.org/10.1095/biolreprod.115.128314>

BioOne Complete (complete.BioOne.org) is a full-text database of 200 subscribed and open-access titles in the biological, ecological, and environmental sciences published by nonprofit societies, associations, museums, institutions, and presses.

Your use of this PDF, the BioOne Complete website, and all posted and associated content indicates your acceptance of BioOne's Terms of Use, available at www.bioone.org/terms-of-use.

Usage of BioOne Complete content is strictly limited to personal, educational, and non - commercial use. Commercial inquiries or rights and permissions requests should be directed to the individual publisher as copyright holder.

BioOne sees sustainable scholarly publishing as an inherently collaborative enterprise connecting authors, nonprofit publishers, academic institutions, research libraries, and research funders in the common goal of maximizing access to critical research.

Novel Technique for Visualizing Primordial Germ Cells in Sturgeons (*Acipenser ruthenus*, *A. gueldenstaedtii*, *A. baerii*, and *Huso huso*)¹

Taiju Saito² and Martin Psenicka

Laboratory of Germ Cells, Research Institute of Fish Culture and Hydrobiology, South Bohemian Research Center of Aquaculture and Biodiversity of Hydrocenoses, Faculty of Fisheries and Protection of Waters, University of South Bohemia in Ceske Budejovice, Vodnany, Czech Republic

ABSTRACT

Primordial germ cells (PGCs) are the origin of all germ cells in developing embryos. In the sturgeon embryo, PGCs develop from the vegetal hemisphere, which mainly acts as an extraembryonic source of nutrition. Current methods for studying sturgeon PGCs require either killing the fish or using costly and time-consuming histological procedures. Here, we demonstrate that visualization of sterlet (*Acipenser ruthenus*) PGCs in vivo is feasible by simply labeling the vegetal hemisphere with fluorescein isothiocyanate (FITC)-dextran. We injected FITC-dextran, with molecular weights varying between 10 000 and 2 000 000, into the vegetal pole of 1- to 4-cell stage embryos. At the neurula to tail-bud developmental stages, FITC-positive PGC-like cells appeared ventrally around the developing tail bud in the experimental group that received a high-molecular-weight FITC-dextran. The highest average number of FITC-positive PGC-like cells was observed in embryos injected with FITC-dextran having a molecular weight of 500 000 (FD-500). The pattern of migration of the labeled cells was identical to that of PGCs, clearly indicating that the FITC-positive PGC-like cells were PGCs. Labeled vegetal cells, except for the PGCs, were digested and excreted before the embryos starting feeding. FITC-labeled PGCs were observed in the developing gonads of fish for at least 3 mo after injection. We also found that FD-500 could be used to visualize PGCs in other sturgeon species. To the best of our knowledge, this report is the first to demonstrate in any animal species that PGCs can be visualized in vivo for a long period by the injection of a simple reagent.

developmental biology, early development, fish reproduction, gonad development, primordial germ cells, sturgeon

INTRODUCTION

In fish ontogenesis, the origin of all germ cells can be traced back to several dozen primordial germ cells (PGCs) in the developing embryo. In fish, PGCs form at various locations by the inheritance of maternally supplied “germplasm” (a

particular region of cytoplasm that specifies germ cell fate) and then migrate toward the place where the gonad will develop. PGCs are the basic germinal elements of the developing gonad, and the developmental integrity of PGC formation, migration, and proliferation is essential for gametogenesis in the sexually mature individual [1]. Elucidation of the development of PGCs in fish will provide fundamental insights regarding gonad development, sex determination, and sexual differentiation as well as a promising technique to manipulate the reproductive system of fishes [2, 3].

The ability to track PGC development is recognized as important in the management of some animals. For example, PGCs appear to play an important role in sexual differentiation, and the absolute number of PGCs may determine sexual phenotype in some teleosts [4–6]. Moreover, PGC migration during embryonic development can be disrupted by environmental conditions, such as low dissolved oxygen in the culture water [7]. These characteristics of PGCs have stimulated research concerning their role in gonadal formation and sex determination in a variety of model fish species [8–11]. The information obtained in such studies is also very important for the management and conservation of endangered species, such as sturgeons.

Sturgeons belong to the order Acipenseriformes, which is one of the oldest in the class Actinopterygii. This order is frequently referred to as “living fossils” in the literature [12]. Sturgeons receive considerable attention across a wide range of disciplines because of their commercial importance as a source of caviar and because they are all imperiled as a result of habitat alteration and overharvesting within much of their ranges [13]. Despite its importance, however, PGC development in the embryos and fry of sturgeon species has been investigated little until recently, although Grandi et al. [14] have provided histological observations on late embryonic developmental stages. Sturgeon eggs have holoblastic cleavage, similar to that in anurans [15]. The pattern of development of sturgeon embryos more closely resembles that of *Xenopus* than of teleost species, not only in their cleavage pattern but also in many other aspects [16, 17]. The sturgeon egg is relatively large and contains considerable quantities of lipids; because of these properties, it is difficult to distinguish PGCs from somatic cells in early embryos using standard methods, such as histology. Recently, however, we investigated PGC development in sturgeon embryos in vivo using injection of an artificial mRNA (*gfp-nos3* 3′-untranslated region [UTR] mRNA) and demonstrated that PGCs originated from the presumptive extraembryonic tissue located at the vegetal pole [18]. Thus, the origin of the PGCs is spatially distant from the somatic cells of the early embryo, and the two are somewhat separated by the vegetal extraembryonic tissue (yolk-blastomeres). During embryonic development, PGCs migrate from their place of origin to the gonadal region. Unfortunately, using

¹Supported by the Ministry of Education, Youth, and Sports of the Czech Republic; projects “CENAKVA” (South Bohemian Research Center of Aquaculture and Biodiversity of Hydrocenoses; CZ.1.05/2.1.00/01.0024) and “CENAKVA II” (LO1205 under the NPU I program); and the Czech Science Foundation (P502/13/26952S).

²Correspondence: Taiju Saito, Nishiura Station, South Ehime Fisheries Research Center, Ehime University, 25-1 Uchidomari, Ainan-cho, Ehime 798-4206, Japan. E-mail: taiju76@gmail.com

Received: 16 January 2015.

First decision: 19 February 2015.

Accepted: 3 June 2015.

© 2015 by the Society for the Study of Reproduction, Inc.

This is an Open Access article, freely available through *Biology of Reproduction's* Authors' Choice option.

eISSN: 1529-7268 <http://www.biolreprod.org>

ISSN: 0006-3363

the *gfp-nos3* 3'-UTR mRNA approach, green fluorescent protein (GFP) expression in the PGCs gradually disappears after hatching and becomes difficult to observe after approximately 1 mo postfertilization. In addition to this technical limitation, the mRNA construct used in the injection requires many steps for the preparation of nucleotides as well as RNase-free conditions. Currently, transgenic strains that possess a reporter gene in germ cells are not available in sturgeons, largely because of the extremely long reproductive cycle. In light of the problems outlined above, new approaches are needed to enable visualization of sturgeon PGCs in vivo both to study the dynamics of their development and to enable isolation of viable PGCs for other protocols (e.g., cryopreservation, cell culture, or cell transplantation). These new methodologies will preferably be non-RNA based or non-transgene based to reduce costs. Additionally, labeling of PGCs should last longer than 1 mo and allow the cells to be identified in histological sections.

In the present study, we took advantage of the pattern of PGC development in a sturgeon species to visualize PGCs using an injection with a fluorescent tracer dye conjugated to high-molecular-weight dextran (fluorescein isothiocyanate [FITC]-dextran). The concept of this approach was to label the germplasm region, where PGCs are exclusively generated, and thereby to label the PGCs. We found that injection of FITC-dextran into the vegetal pole at an early cleavage stage labels the vegetal yolk-blastomeres as well as the FITC-positive PGCs, which have been formed in this region, before they migrate toward the genital ridge. The vegetal cells of this area are mainly digested to provide nutrition via the newly formed gut. To the best of our knowledge, this is the first report that PGCs of any animal species can be labeled in vivo by a non-molecular biological technique.

MATERIALS AND METHODS

Ethics

All experimental procedures were performed in accordance with national and institutional guidelines on animal experimentation and care and were approved by the Animal Research Committee of the University of South Bohemia in Ceske Budejovice.

Preparation of Embryos

In the present study, we used embryos from pairs of sterlet (*Acipenser ruthenus*), Russian sturgeon (*A. gueldenstaedtii*), Beluga sturgeon (*Huso huso*), and Siberian sturgeon (*A. baerii*). The fish were held in tanks at 15°C. To induce spermiogenesis, males were injected with a single intramuscular injection of 40 mg/kg of acetone-dried carp pituitary homogenized extract (CPE). At 42 h after hormonal injection, sperm were collected from the urogenital papilla using a catheter, transferred to a separate cell-culture container (250 ml), and stored at 4°C until use. In females, ovulation was induced with two acetone-dried CPE injections, the first of 0.5 mg/kg and the second, 12 h later, of 45 mg/kg. The ovulated eggs were collected 42 h after the first injection. The eggs were fertilized with sperm in dechlorinated water at 15°C. Fertilized eggs become sticky when they come in contact with water, and the sticky chorion makes it difficult to manipulate and cultivate the eggs. To remove the stickiness of the outer layer, the eggs were treated with 0.1% tannic acid solution (three times in 10 min). Then, the outermost layer of the chorion was removed using forceps, and the embryos were cultured in dechlorinated tap water containing 0.01% penicillin and 0.01% streptomycin at 15°C until hatching. Up to 20 embryos were kept in 100 ml of dechlorinated tap water, and the water was replaced every 24 h. We used the description of development by Ginsburg and Dettlaff [19] to stage prelarvae.

Microinjections

Three injection experiments were conducted as follows: First, to test whether it was possible to confine the area of labeling in an embryo by changing the molecular weight of the tracer dye, we coinjected 5%

tetramethylrhodamine (TRITC)-dextran (molecular weight, 10 000; TD-10) and 5% FITC-dextran (molecular weight, 500 000; FD-500) in 0.2 M KCl into the vegetal pole of 1-cell stage fertilized embryos. Second, to determine the optimal size of dextran molecule for FITC-labeling of PGCs, we injected FITC-dextran of five different molecular weights into the vegetal pole of 1- to 4-cell stage embryos. The average molecular weight of each FITC-dextran was 10 000 (FD-10), 70 000 (FD-70), 250 000 (FD-250), 500 000 (FD-500), and 2 000 000 (FD-2000) (all from Sigma). All FITC-dextran were dissolved in 0.2 M KCl at 5% concentration. Third, as positive control, we synthesized *gfp-nos3* 3'-UTR mRNA for injection into the vegetal pole of fertilized embryos at the 1- to 4-cell stage. The capped sense mRNA was synthesized in vitro using the mMESSAGE mMACHINE Kit (Ambion) and dissolved at 500 µg/µl in 0.2 M KCl.

The amount of all solutions injected into each egg could not be measured accurately because of interference by the pigment layer with observation of the egg cytoplasm to standardize the injection pressure. Therefore, we injected the solution by initiating a low, constant flow from the tip of the needle before inserting the needle into the egg. Each embryo was observed just after injection using the Leica M165 fluorescence stereomicroscope imaging system to determine whether it had FITC-labeled PGCs; nonlabeled eggs were discarded. The number of PGCs in each embryo was counted using the fluorescence stereomicroscope during stages 24–26 (lateral plate fusion). Three replicated experiments were performed for each experimental group, and the average number of PGCs was calculated from the sum of these experiments. PGC-positive embryos were placed in a 1% agar-coated dish in a tricaine solution (33.6 mg in 100 ml of water) to anesthetize, and images were captured using the Leica M165 imaging system. The captured images were quantified and processed using ImageJ (National Institutes of Health) or Photoshop CS5.1 (Adobe).

Immunostaining of FITC-Labeled Cells

The FITC-labeled PGC-like cells were manually isolated from the tail bud-stage embryos. These cells were fixed with 4% paraformaldehyde on a glass slide that was treated with poly-L-lysine for 1 h at 4°C. Permeabilization of the cells was performed three times with 0.3% Triton X-100 in PBS for 10 min each time. Cells were washed three times in PBS and then subjected to the blocking treatment with 1% bovine serum albumin (BSA) and 0.05% Tween in PBS for 30 min. Then, cells were incubated in anti-DDX4 antibody (600-fold dilution; 1% BSA and 0.05% Tween in PBS; GeneTex, Inc.) for 2 h at room temperature. After washing three times with 1% BSA and 0.05% Tween in PBS for 5 min each time, cells were incubated in anti-rabbit immunoglobulin G-TRITC antibody (400-fold dilution; 1% BSA and 0.05% Tween in PBS; Sigma-Aldrich) for 1 h at room temperature. Cells were washed three times with PBS. Before observation, cells were stained for 10 min with 4',6-diamidino-2-phenylindole (DAPI; 50 µg/ml) for visualization of nuclei. After washing three times with PBS, cells were observed and photographed using an Olympus IX83 microscope equipped with a digital camera ORCA-R2 (Hamamatsu Photonics). Multicolor images were processed and merged into single images using cellSens software (Olympus).

Time-Lapse Imaging

Sturgeon embryos that had FITC-labeled PGCs following FD-500 injection were placed in a 120-mm dish filled with 3% methylcellulose (Sigma) in water for time-lapse imaging (Leica M165 and Leica Application suite [LAS] software version 3.1). Images were captured at 30-sec intervals for 3 h at room temperature (adjusted to 18°C using an air conditioner). The speed of cell migration was calculated from the cell paths. Cell centroid movements were tracked at 5-min intervals over an 80-min period using ImageJ software, and mean migration speeds were compared using *t*-tests.

FITC-Labeled PGCs in Fry

The PGC-labeled embryos following FD-500 injection were placed in an aquarium after hatching and fed with tubefex and dried pellets two to three times per day. Some embryos were killed using a tricaine overdose and cervical dislocation. The abdomens were then opened to analyze their genital ridges to determine how long FITC fluorescence in the PGCs lasted after the hatching stage.

Histological Observations

Embryos with labeled PGCs following FD-500 injection (FITC-500 embryos) were allowed to develop to the hatching stage and then fixed

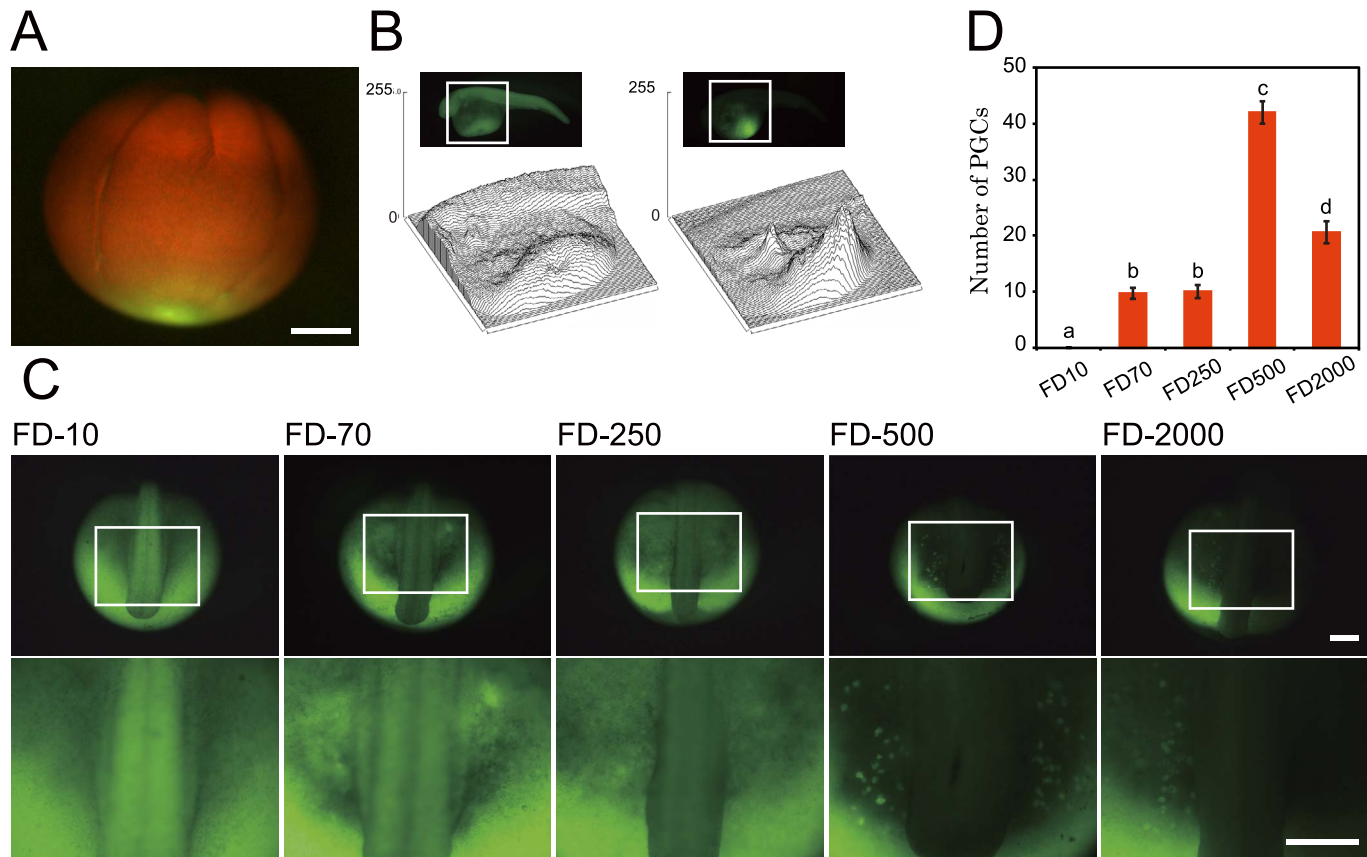


FIG. 1. Distribution of tracer dyes with different molecular weights in *Acipenser ruthenus* embryos. **A)** Lateral view of a 4-cell stage embryo colabeled with TD-10 and FD-500 at the 1-cell stage. **B)** Three-dimensional histogram of FD-10 (**left**) and FD-500 (**right**) distribution in stage-32 embryos. The histograms were obtained from the boxed areas in the upper images. Note that the distribution of FITC is confined to the yolk region in the FD-500-injected embryo. **C)** Posterior views of embryos labeled with FITC-dextrans of different molecular weights. Lower images show magnified views of the boxed areas in the upper images. **D)** Average number of PGCs labeled with FITC-dextrans of different molecular weights at early tail-bud stage (stage 26 or 27). Vertical bars indicate standard deviations. Means with different letters in are significantly different ($P < 0.05$ by Kruskal-Wallis test and Scheffe test). Bar = 500 μ m.

overnight as larvae in Bouin fixative and embedded in paraffin. Serial sections were cut at 8 μ m thickness and attached to glass microscope slides with 0.01% poly-L-lysine. FITC labeling was detected using an anti-FITC antibody (71-1900; Invitrogen) and visualized with diaminobenzidine by the ABC reaction (VECTASTAIN ABC kit; Vector Laboratories) as described in the manufacturer's protocol; the sections were counterstained with hematoxylin-and-eosin. For cryosections, FITC-500 embryos were fixed in 4% paraformaldehyde in PBS for 1 h, washed in PBS three times for 10 min each time, embedded in Tissue-Tek O.C.T. (Sakura), and rapidly frozen in a -80°C deep freezer. Sections of 10 μ m thickness were cut using a CM 1850 cryostat (Leica) at -20°C and placed on Superfrost microscope slides (Fisher Scientific). The specimens were mounted in 0.1% DAPI solution in PBS and then photographed using the Olympus IX83 microscope equipped with a digital camera ORCA-R2 (Hamamatsu Photonics).

RESULTS

Diffusion Speed of Tracer Dyes with Different Molecular Weights

We coinjected TD-10 and FD-500 into the vegetal pole of fertilized embryos to compare the diffusion speed of each molecules. Up until the 4-cell stage, TD-10 permeated rapidly to the animal pole, whereas FD-500 remained in the area near the vegetal pole (Fig. 1A). The speed of diffusion of FD-500 was very slow, and as the embryos developed, cleavage planes isolated the animal hemisphere before the FITC was able to enter. Consequently, in the stage-32 embryo (tip of tail touches the head), high-molecular-weight FITC-dextran was confined to the labeled area of yolk cells (Fig. 1B).

Optimal Molecular Weight for Labeling PGCs

We injected FITC-dextrans of five different molecular weights into the vegetal pole of 1- to 4-cell stage embryos to determine the optimal dextran molecule size for FITC labeling of PGCs. As anticipated, the spread of the FITC-dextran from the injection site varied according to its molecular weight; that is, larger-molecular-weight FITC-dextran was confined to a smaller area (Fig. 1C). FITC-positive PGC-like cells appeared around the margins of the tail bud (Fig. 1C). At this embryonic stage (stage 24–26), the highest average number of PGC-like cells was seen in the embryos injected with FD-500 (mean \pm SD: 42.0 ± 27.8) (Fig. 1D). By contrast, no PGC-like cells could be distinguished at any stage in FD-10-labeled embryos because all cells were positive for FITC (Fig. 1C).

Vasa Protein Expression in FITC-Labeled Cells

Next, we analyzed the pattern of migration of PGC-like cells in embryos to determine whether FD-500-labeled PGC-like cells were indeed PGCs. Serial observations and time-lapse imaging under a fluorescence stereomicroscope demonstrated that the route and behavior of the PGC-like cells were identical to those of PGCs and that their final location was at the position where the gonads develop (Fig. 2, A and B). To address whether the FITC-labeled PGC-like cells express germline specific protein, we performed anti-Vasa (DDX4)

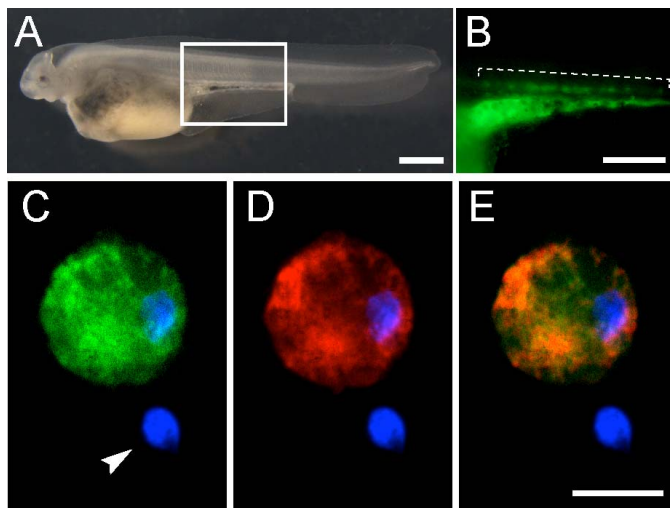


FIG. 2. The PGC-like cells migrated toward the genital ridge in a same way as PGCs and expressed Vasa protein in *Acipenser ruthenus*. **A)** An FD-500-labeled embryo at stage 36. **B)** A fluorescent image of a box in **A**. Broken line shows PGCs. **C)** FITC-positive cell and FITC-negative cell stained with DAPI. Arrowhead shows a nucleus of the FITC-negative cell. **D)** DDX4 expression visualized by TRITC. **E)** Merged image of **C** and **D**. Bar = 1 mm (**A**), 500 μ m (**B**), and 20 μ m (**D**).

antibody staining. Vasa protein expression was observed in the FITC-positive PGC-like cells at the tail-bud stage (Fig. 2, C–E), whereas non-FITC-labeled cells showed low or no Vasa protein expression. Our analysis therefore showed that the PGC-like cells were in fact PGCs.

Migration of FITC-Labeled PGCs in Embryos

The time-lapse imaging analysis indicated that migration of sturgeon PGCs had two phases. At around stage 25, the PGCs were active and developed protrusions or pseudopodia (Fig. 3A, red arrowhead). These PGCs could be removed with comparative ease from surrounding tissues by surgical manipulation with forceps. However, the speed of migration of the cells declined until around stage 32 or 33. These cells did not change their positions in relation to other PGCs, and all continued to move slowly and gradually toward the future gonad (Fig. 3, B and C). After the end of this phase (around stages 34–36; hatching), PGCs were found to be tightly attached to and surrounded by somatic cells on the developing gut; mechanical isolation of these cells was difficult (Fig. 3D).

Longevity of FITC Labeling During Sturgeon Development

No significant differences in survival rates among the control and two experimental groups were found (Table 1). We were able to identify FITC-positive PGCs for at least 3 mo after fertilization using a stereomicroscope (Fig. 4, A–E) and to assess their rate of proliferation by counting the number of FITC-positive cells (Fig. 4F). By contrast, GFP-labeled PGCs

TABLE 1. Survival rates of *Acipenser ruthenus* embryos injected with different tracers at the hatching stage.

Treatment	Total embryos (n)	Hatched embryos (n [%])	Dead (n [%])
Control	50	46 (92.0)	4 (8.0)
FD-500	102	92 (90.2)	10 (9.8)
<i>gfp-nos3</i> 3'-UTR mRNA	107	100 (93.5)	7 (6.5)

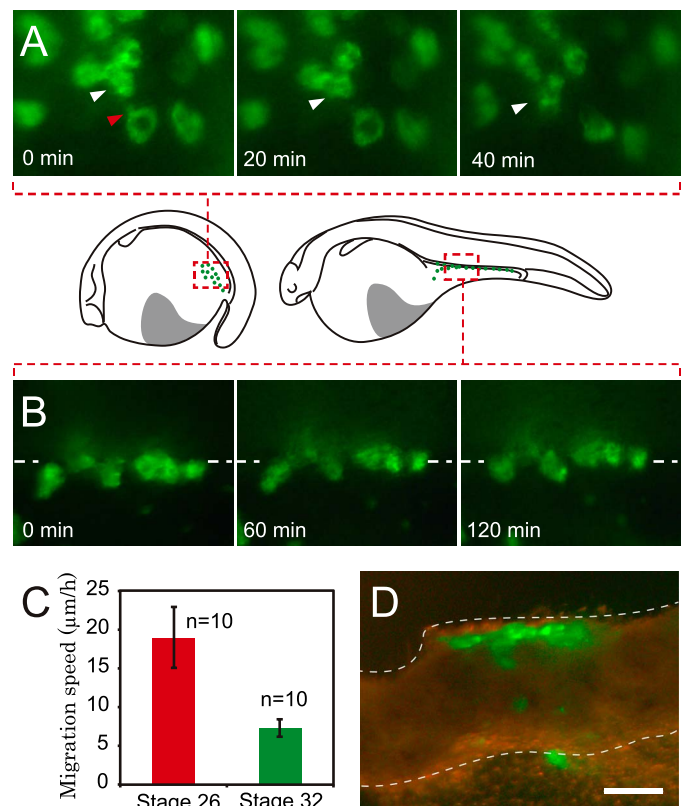


FIG. 3. Migration speed of PGCs slow down as the *Acipenser ruthenus* embryo develops. **A)** Migration of PGCs at stages 26 and 27. The PGCs show active migration (see the cell indicated by the white arrowhead) and show protrusions (red arrowhead). **B)** At approximately stage 32, PGCs do not show active migration, but they do gradually move dorsally. Broken lines indicate the border between the embryonic body and the yolk extension. **C)** Comparison of average migration speeds of PGCs at stages 26 and 32. Vertical bar indicates standard deviations. The means were significantly different ($P < 0.0001$ by an unpaired *t*-test). **D)** An isolated gut with FITC-positive PGCs from a stage-34 to stage-35 embryo (around hatching stage). Broken lines indicate the outlines of the gut. Bar = 100 μ m.

were difficult to observe after hatching and had completely disappeared before the age of 2 mo (Fig. 4F).

Injection of TRITC-dextran (molecular weight, 500 000; TD-500) also successfully labeled PGCs in the same manner as FD-500. Moreover, the FD-500/TD-500 PGC visualization technique also worked in other sturgeon species, such as Russian sturgeon, Beluga sturgeon, and Siberian sturgeon.

Histological Detection of Injected FITC in Embryos

The FITC-labeled cells could be detected in paraffin-mounted histological sections using an anti-FITC antibody and diaminobenzidine staining. In the sections, the FD-500-labeled PGCs were seen as brown cells at the genital ridge of hatched larvae (Fig. 5, A and B). The FITC-labeled PGCs were also observed in cryosections at 90 days postfertilization (dpf) (Fig. 5, C and D). At this stage, PGCs were completely surrounded in the gonad by somatic cells. These results support our conclusion that FITC-labeled PGC-like cells are genuine PGCs.

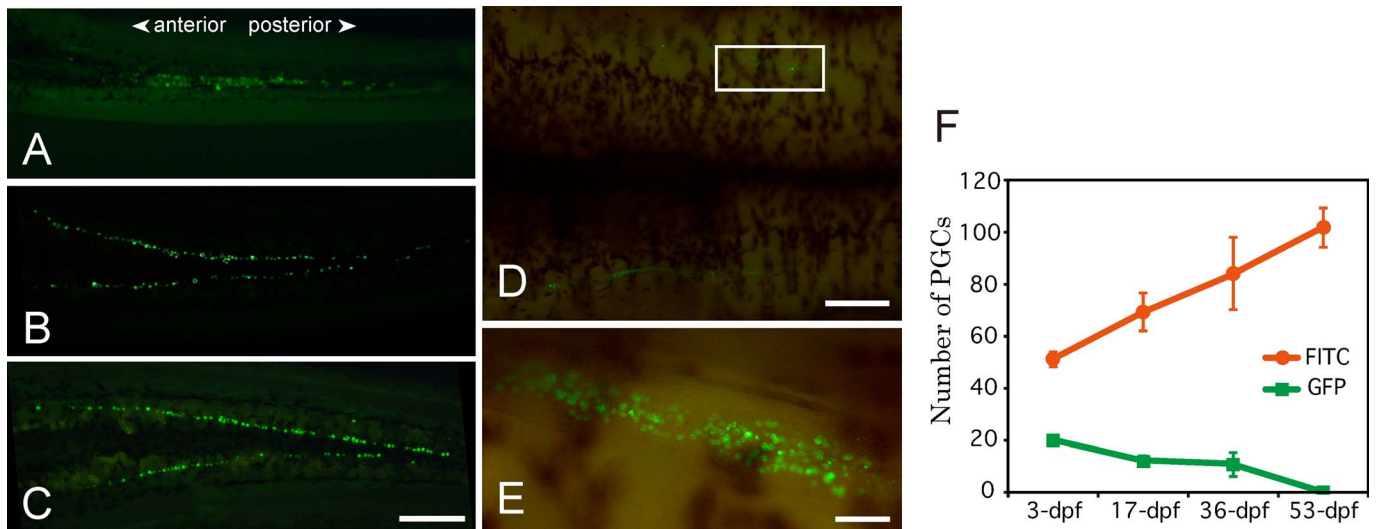


FIG. 4. PGC visualization during genital ridge formation in *Acipenser ruthenus*. **A–D**) Ventral views of FITC-positive PGCs in the upper parts of the abdominal cavity after removal of the intestines in 17-dpf (**A**), 36-dpf (**B**), 53-dpf (**C**), and 90-dpf (**D**) embryos, respectively. **E**) Magnified image of the boxed area in **D**. The mingled PGCs in the upper part of the body cavity of the 17-dpf embryo separate into two lines as the fish develop. **F**) Comparison of the average number of PGCs visualized by FD-500 or *gfp-nos3* 3'-UTR at each developmental stage. Vertical bars indicate standard deviations. Bar = 500 μ m (**C** and **D**) and 100 μ m (**E**).

DISCUSSION

In the present study, we demonstrated that in sturgeon zygotes injected at the 1- to 4-cell stage with FITC or TRITC conjugated with a high-molecular-weight dextran (FD-500/TD-500), PGCs could be visualized from the neurula to tail-bud stage (stage 21–24) until at least 3 mo of age. This nontransgenic PGC-labeling technique provides significant experimental benefits for investigating PGC biology in *Acipenseridae* species compared to previously developed approaches. Transgenic strains that carry a fluorescent protein in their germ cells provide a valuable tool for research and have been established in zebrafish, medaka, and trout [20–22]. Because reproduction in *Acipenseridae* species only occurs at 5 to 20 yr of age, depending on the species, establishing transgenic strains would require between 10 and 40 yr (a minimum of two generations) for selection. Furthermore, the selection and maintenance of transgenic sturgeon would necessitate the use of very large holding facilities, and approval would be required for breeding genetically modified organisms. The alternative approach of injecting mRNA to enable PGC visualization has also been reported in some fish and allows investigation of PGC development in these species [18, 23–26]. However, we found that GFP expression in PGCs after injection of *gfp-nos3* 3'-UTR mRNA did not last more than 2 mo in sturgeon, probably because the injected mRNA was gradually degraded during PGC development. In zebrafish, the expression of *nanos3* (*nos3*) mRNA declines to an undetectable level by 5 dpf and remains so until 21 dpf; subsequently, the gene is expressed again, but only in early oocytes of females [23, 27]. Furthermore, the mRNA injection technique needs more preparative steps and requires increased cost and time. In contrast, the PGC visualization technique using FD-500/TD-500 is simpler than production of transgenic fish and is more stable and affordable than use of GFP expression after mRNA injection. Even though the level of FITC fluorescence gradually declined as the cells proliferated, it was easy to follow the course of PGC development.

In some fish species, such as zebrafish, medaka, and stickleback, the number of PGCs likely plays an important role

in sexual differentiation. In these species, female PGCs appear to proliferate more rapidly than male PGCs [4–6, 28], although in loach (*Misgurnus anguillicaudatus*) and goldfish (*Carassius auratus auratus*), the number of PGCs does not affect sexual differentiation [10, 11]. Considerable interest exists in understanding the sex determination mechanism in sturgeons, mainly because of the demand for monosex populations of caviar-producing females. Although some studies have provided evidence of a ZW-female heterogametic genetic sex determination system [29, 30], it remains uncertain whether the germ cells or gonadal somatic cells predominantly determine primary gonadal sex. The present study clearly shows that the

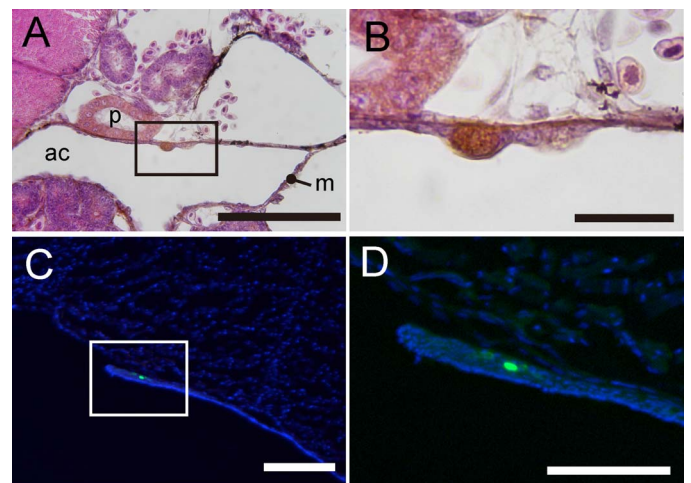


FIG. 5. Detection of FITC-labeled PGCs in *Acipenser ruthenus* on histological sections. **A** and **B**) Paraffin section of a 1-mo-old fry with FITC-positive PGCs stained with an anti-FITC antibody and diaminobenzidine. **B**) A magnified image of the boxed area in **A**. The brown labeled cell is the PGC. **C** and **D**) Cryosection of the gonadal anlage of a 90-dpf embryo. **D**) A magnified image of the boxed area in **C**. Blue dots are DAPI-stained nuclei. FITC-labeled PGCs are enclosed in genital somatic cells and are proliferating. ac, abdominal cavity; m, mesenchyme; p, pronephric duct. Bar = 50 μ m (**A**), 10 μ m (**B**), 200 μ m (**C**), and 100 μ m (**D**).

proliferation of PGCs in the genital ridges can be observed using FITC fluorescence. Thus, if dimorphism in PGC proliferation rates exists between females and males, we should be able to identify this effect in sturgeon. The present study throws no light on this matter because a comparatively small sample of embryos was analyzed; however, counting PGCs in sturgeon will provide some indication of the likely sexual differentiation mechanism in these species.

The number of labeled PGCs varied with the molecular weight of the FITC-dextran. Interestingly, the efficiency of PGC visualization using FD-500 was higher than that with FD-2000. This suggests that the area in which PGCs are formed at the vegetal region is larger than that labeled by FD-2000. In support of this conclusion, it was reported that formation of GFP islands after injection of *gfp-buc* mRNA is observed distant to the vegetal pole [18]. Germplasm likely accumulates in a wide area of the vegetal hemisphere in sturgeon. Elucidation of the process of PGC formation in sturgeon will require investigation of the distribution of germplasm in eggs.

We applied time-lapse imaging analysis to FITC-positive PGCs during embryonic development and demonstrated that migration of the PGCs could be divided into two phases, active and slow migration, at different developmental stages. PGCs in the active migration phase were easily isolated surgically, whereas PGCs at the later stages were difficult to isolate because of a close interaction with the surrounding mesodermal tissue. We suggest that sturgeon PGCs at later developmental stages migrate in a coordinated manner with the mesodermal somatic tissue on the developing gut. In support of this conclusion, it has been reported in the Adriatic sturgeon (*Acipenser naccarii*) that each PGC is located near the mesentery at around the hatching stage and is surrounded by thin, cytoplasmic extensions from two or three somatic cells [14]. In medaka, migrating PGCs are surrounded by mesodermal somatic cells when they are located around the upper part of the developing gut until 7 dpf, and then they move toward the genital ridge [31]. However, in Nibe croaker (*Nibea mitsukurii*), PGCs appear to be enclosed by genital somatic cells after passing through the mesentery of the dorsal wall of the body cavity where the gonad forms [32]. Gonad development requires coordinated soma-germline interactions that ensure proper development and function of the gametes. The interaction of PGCs and somatic cells during their migration in sturgeon will be studied further using the FITC-labeling technique.

The present results and our previous reports indicate that techniques for “surrogate production” in sturgeon are becoming more and more practicable (see reviews, see [3, 33–35]). We have already shown that sturgeon PGCs can be isolated using an enzymatic solution and that the isolated cells can be transplanted into different species; furthermore, transplanted PGCs can migrate to the genital ridge even in a phylogenetically distant xenogeneic host [18]. Additionally, we established a technique for isolating spermatogonia and oogonia using Percoll gradient layers; transplantation of these cells into the body cavity of hatched larvae showed that they can proliferate, migrate, and settle at the host gonadal ridge [36]. In this transplantation experiment, the PGCs of the host were labeled with FITC, whereas the transplanted donor germ cells were labeled with the common cell-labeling reagent PKH-26; this allowed us to check that the donor PGCs localized to the developing host gonad. The next step in advancing this technology will be to remove endogenous germ cells (i.e., sterilization of the host). Strategies for host sterilization have been reported in many species, such as busulfan treatment combined with high water temperatures to kill spermatogonia/

oogonia in adult fish [37, 38] or blocking gametogenesis by producing triploid or hybrid fish [39, 40]. To date, however, complete removal of germ cells seems to have been achieved only in fish where PGC development was blocked by a gene knockdown [10, 11, 41, 42]. To achieve this in sturgeon, genome editing techniques using CRISPR/Cas9 or TALEN could be applied to produce sterilized fish by knocking down PGC-specific genes. The FITC-labeling technique for PGCs described here will be of value for monitoring successful induction of sterility after inhibiting/disturbing PGC development.

In conclusion, we have developed a technique to visualize PGCs in sturgeon embryos. Visualization of PGCs has great potential for the investigation of PGC development, including their migration and proliferation patterns in embryos, hatched larvae, and young fry. Our new technique might also be used to visualize PGCs in species that have a pattern of PGC development similar to that of sturgeon, such as *Eleutherodactylus coqui* [43, 44]. Furthermore, we believe our new technique will be an invaluable tool for developing surrogate production in sturgeon.

ACKNOWLEDGMENT

We wish to thank Dr. W.L. Shelton for his valuable comments and English correction during preparation of the manuscript. We are also grateful to Dr. M. Rodina, Dr. D. Gela, and the members of the Laboratory of Germ Cells, Faculty of Fisheries and Protection of Waters, University of South Bohemia in Ceske Budejovice for their support on experiments.

REFERENCES

1. Ewen-Campen B, Schwager EE, Extavour CGM. The molecular machinery of germ line specification. *Mol Reprod Dev* 2009; 77:3–18.
2. Yoshizaki G, Takeuchi Y, Kobayashi T, Takeuchi T. Primordial germ cell: a novel tool for fish bioengineering. *Fish Physiol Biochem* 2003; 28: 453–457.
3. Yamaha E, Saito T, Goto R, Arai K. Developmental biotechnology for aquaculture, with special reference to surrogate production in teleost fishes. *J Sea Res* 2007; 58:8–22.
4. Lewis ZR, McClellan MC, Postlethwait JH, Cresko WA, Kaplan RH. Female-specific increase in primordial germ cells marks sex differentiation in threespine stickleback (*Gasterosteus aculeatus*). *J Morphol* 2008; 269: 909–921.
5. Saito D, Morinaga C, Aoki Y, Nakamura S, Mitani H, Furutani-Seiki M, Kondoh H, Tanaka M. Proliferation of germ cells during gonadal sex differentiation in medaka: insights from germ cell-depleted mutant *zenzai*. *Dev Biol* 2007; 310:280–290.
6. Tzung K-W, Goto R, Saju JM, Sreenivasan R, Saito T, Arai K, Yamaha E, Hossain MS, Calvert MEK, Orban L. Early depletion of primordial germ cells in zebrafish promotes testis formation. *Stem Cell Rep* 2015; 4:61–73.
7. Lo K, Hui M, Yu RMK, Wu R. Hypoxia impairs primordial germ cell migration in zebrafish (*Danio rerio*) embryos. *PLOS ONE* 2011; 6: e24540.
8. Slanchev K, Stebler J, de la Cueva-Méndez G, Raz E. Development without germ cells: the role of the germ line in zebrafish sex differentiation. *Proc Natl Acad Sci U S A* 2005; 102:4074–4079.
9. Kurokawa H, Saito D, Nakamura S, Katoh-Fukui Y, Ohta K, Baba T, Morohashi K-I, Tanaka M. Germ cells are essential for sexual dimorphism in the medaka gonad. *Proc Natl Acad Sci U S A* 2007; 104:16958–16963.
10. Fujimoto T, Nishimura T, Goto R, Kawakami Y, Yamaha E, Arai K. Sexual dimorphism of gonadal structure and gene expression in germ cell-deficient loach, a teleost fish. *Proc Natl Acad Sci U S A* 2010; 107: 17211–17216.
11. Goto R, Saito T, Takeda T, Fujimoto T, Takagi M, Arai K, Yamaha E. Germ cells are not the primary factor for sexual fate determination in goldfish. *Dev Biol* 2012; 370:98–109.
12. Grande L, Bemis WE. Osteology and phylogenetic relationships of fossil and recent paddlefishes (Polyodontidae) with comments on the interrelationships of Acipenseriformes. *J Vertebr Paleontol* 1991; 11:1–121.
13. The IUCN Red List of Threatened Species, Version 2014.3 [Internet]. Cambridge, UK: International Union for Conservation of Nature and

- Natural Resources. <http://www.iucnredlist.org>. Accessed 19 November 2014.
14. Grandi G, Chicca M. Histological and ultrastructural investigation of early gonad development and sex differentiation in Adriatic sturgeon (*Acipenser naccarii*, Acipenseriformes, Chondrostei). *J Morphol* 2008; 269: 1238–1262.
 15. Elinson RP. Nutritional endoderm: a way to breach the holoblastic-meroblastic barrier in tetrapods. *J Exp Zool* 2009; 312B:526–532.
 16. Ballard WW, Ginsburg AS. Morphogenetic movements in acipenserid embryos. *J Exp Zool* 1980; 213:69–103.
 17. Bolker JA. Gastrulation and mesoderm morphogenesis in the white sturgeon. *J Exp Zool* 1993; 266:116–131.
 18. Saito T, Pšenička M, Goto R, Adachi S, Inoue K, Arai K, Yamaha E. The origin and migration of primordial germ cells in sturgeons. *PLOS ONE* 2014; 9:e86861.
 19. Ginsburg AS, Dettlaff TA. The Russian sturgeon *Acipenser guldensadti*. Part 1. Gametes and early development up to time of hatching. In: Dettlaff TA, Vassetzky SG (eds.), *Animal Species for Developmental Studies*, vol 2, Vertebrates. New York: Springer; 1991:16–65.
 20. Krövel AV, Olsen LC. Expression of a *vas::EGFP* transgene in primordial germ cells of the zebrafish. *Mech Dev* 2002; 116:141–150.
 21. Tanaka M, Kinoshita M, Kobayashi D, Nagahama Y. Establishment of medaka (*Oryzias latipes*) transgenic lines with the expression of green fluorescent protein fluorescence exclusively in germ cells: a useful model to monitor germ cells in a live vertebrate. *Proc Natl Acad Sci U S A* 2001; 98:2544–2549.
 22. Yoshizaki G, Takeuchi Y, Sakatani S, Takeuchi T. Germ cell-specific expression of green fluorescent protein in transgenic rainbow trout under control of the rainbow trout *vasa*-like gene promoter. *Int J Dev Biol* 2000; 44:323–326.
 23. Köprunner M, Thisse C, Thisse B, Raz E. A zebrafish *nanos*-related gene is essential for the development of primordial germ cells. *Gene Dev* 2001; 15:2877–2885.
 24. Yoshizaki G. Green fluorescent protein labeling of primordial germ cells using a nontransgenic method and its application for germ cell transplantation in Salmonidae. *Biol Reprod* 2005; 73:88–93.
 25. Kurokawa H, Aoki Y, Nakamura S, Ebe Y, Kobayashi D, Tanaka M. Time-lapse analysis reveals different modes of primordial germ cell migration in the medaka *Oryzias latipes*. *Dev Growth Differ* 2006; 48: 209–221.
 26. Saito T, Fujimoto T, Maegawa S, Inoue K, Tanaka M, Arai K, Yamaha E. Visualization of primordial germ cells in vivo using GFP-*nos1* 3'UTR mRNA. *Int J Dev Biol* 2006; 50:691–699.
 27. Draper B, McCallum CM, Moens CB. *nanos1* is required to maintain oocyte production in adult zebrafish. *Dev Biol* 2007; 305:589–598.
 28. Satoh N, Egami N. Sex differentiation of germ cells in the teleost, *Oryzias latipes*, during normal embryonic development. *J Embryol Exp Morphol* 1972; 28:385–395.
 29. Van Eenennaam AL, Van Eenennaam JP, Medrano JF, Doroshov SI. Evidence of female heterogametic genetic sex determination in white sturgeon. *J Hered* 1999; 90:231–233.
 30. Omoto N, Maebayashi M, Adachi S, Arai K, Yamauchi K. Sex ratios of triploids and gynogenetic diploids induced in the hybrid sturgeon, the bester (*Huso huso* female × *Acipenser ruthenus* male). *Aquaculture* 2005; 245:39–47.
 31. Hamaguchi S. A light- and electron-microscopic study on the migration of primordial germ cells in the teleost, *Oryzias latipes*. *Cell Tissue Res* 1982; 227:139–151.
 32. Takeuchi Y, Higuchi K, Yatabe T, Miwa M, Yoshizaki G. Development of spermatogonial cell transplantation in Nibe croaker, *Nibea mitsukurii* (Perciformes, Sciaenidae). *Biol Reprod* 2009; 81:1055–1063.
 33. Okutsu T, Yano A, Nagasawa K, Shikina S, Kobayashi T, Takeuchi Y, Yoshizaki G. Manipulation of fish germ cell: visualization, cryopreservation and transplantation. *J Reprod Dev* 2006; 52:685–693.
 34. Yoshizaki G, Fujinuma K, Iwasaki Y, Okutsu T, Shikina S, Yazawa R, Takeuchi Y. Spermatogonial transplantation in fish: a novel method for the preservation of genetic resources. *Comp Biochem Physiol D Genomics Proteomics* 2011; 6:55–61.
 35. Lacerda SMSN, Costa GMJ, Campos-Junior PHA, Segatelli TM, Yazawa R, Takeuchi Y, Morita T, Yoshizaki G, França LR. Germ cell transplantation as a potential biotechnological approach to fish reproduction. *Fish Physiol Biochem* 2012; 39:3–11.
 36. Pšenička M, Saito T, Linhartová Z, Gazo I. Isolation and transplantation of sturgeon early-stage germ cells. *Theriogenology* 2015; 83:1085–1092.
 37. Lacerda SMSN, Batlouni SR, Costa GMJ, Segatelli TM, Quirino BR, Queiroz BM, Kalapothakis E, França LR. A new and fast technique to generate offspring after germ cells transplantation in adult fish: the Nile tilapia (*Oreochromis niloticus*) model. *PLOS ONE* 2010; 5:e10740.
 38. Majhi SK, Hattori RS, Rahman SM, Strüssmann CA. Surrogate production of eggs and sperm by intrapapillary transplantation of germ cells in cytoablated adult fish. *PLOS ONE* 2014; 18:e95294.
 39. Okutsu T, Shikina S, Kanno M, Takeuchi Y, Yoshizaki G. Production of trout offspring from triploid salmon parents. *Science* 2007; 317:1517.
 40. Wong T-T, Saito T, Crodian J, Collodi P. Zebrafish germline chimeras produced by transplantation of ovarian germ cells into sterile host larvae. *Biol Reprod* 2011; 84:1190–1197.
 41. Ciruna B, Weidinger G, Knaut H, Thisse B, Thisse C, Raz E, Schier AF. Production of maternal-zygotic mutant zebrafish by germ-line replacement. *Proc Natl Acad Sci U S A* 2002; 99:14919–14924.
 42. Saito T, Goto R, Arai K, Yamaha E. Xenogenesis in teleost fish through generation of germ-line chimeras by single primordial germ cell transplantation. *Biol Reprod* 2008; 78:159–166.
 43. Buchholz DR, Singamsetty S, Karadge U, Williamson S, Langer CE, Elinson RP. Nutritional endoderm in a direct developing frog: a potential parallel to the evolution of the amniote egg. *Dev Dyn* 2007; 236: 1259–1272.
 44. Elinson RP, Sabo MC, Fisher C, Yamaguchi T, Orii H, Nath K. Germ plasm in *Eleutherodactylus coqui*, a direct developing frog with large eggs. *EvoDevo* 2011; 2:20.